

Immune Responses in an Infant with Congenital Heart Disease and Severe COVID-19

Paul Licciardi (✉ paul.licciardi@mcri.edu.au)

Murdoch Childrens Research Institute <https://orcid.org/0000-0001-6086-6285>

Danielle Wurzel

Murdoch Children's Research Institute

Melanie Neeland

Murdoch Children's Research Institute <https://orcid.org/0000-0001-7301-9982>

Jeremy Anderson

Murdoch Childrens Research Institute

Yara-Natalie Abo

Murdoch Children's Research Institute

Lien Anh Ha Do

Murdoch Childrens Research Institute

Celeste Donato

Murdoch Children's Research Institute

Julie Bines

Murdoch Children's Research Institute

Zheng Quan Toh

Murdoch Children's Research Institute <https://orcid.org/0000-0002-0282-5837>

Rachel Higgins

Murdoch Children's Research Institute

Sedi Jalali

Murdoch Children's Research Institute

Theresa Cole

Murdoch Children's Research Institute

Kanta Subbarao

University of Melbourne <https://orcid.org/0000-0003-1713-3056>

Alissa McMinn

University of Melbourne

Kate Dohle

Murdoch Children's Research Institute

Gabrielle Haeusler

Murdoch Children's Research Institute

Sarah McNab

Royal Children's Hospital

Annette Alafaci

Murdoch Children's Research Institute

Isabella Overmars

Murdoch Children's Research Institute <https://orcid.org/0000-0002-9710-6113>

Vanessa Clifford

Murdoch Children's Research Institute

Lai-Yang Lee

Murdoch Children's Research Institute

Andrew Daly

The Royal Children's Hospital

Jim Buttery

Murdoch Children's Research Institute

Penelope Bryant

Murdoch Children's Research Institute

David Burgner

Murdoch Children's Research Institute <https://orcid.org/0000-0002-8304-4302>

Andrew Steer

Murdoch Children's Research Institute

Shidan Tosif

Murdoch Children's Research Institute

Igor Konstantinov

Royal Children's Hospital, University of Melbourne

Trevor Duke

Murdoch Children's Research Institute

Dan Pellicci

Murdoch Children's Research Institute

Nigel Crawford

Murdoch Children's Research Institute

Article

Keywords: coronavirus disease-2019 (COVID-19), immune response, infant

Posted Date: April 7th, 2021

DOI: <https://doi.org/10.21203/rs.3.rs-209429/v1>

License:   This work is licensed under a Creative Commons Attribution 4.0 International License.

[Read Full License](#)

Version of Record: A version of this preprint was published at Communications Medicine on November 15th, 2021. See the published version at <https://doi.org/10.1038/s43856-021-00047-7>.

Abstract

Children have lower hospitalisation and mortality rates for coronavirus disease-2019 (COVID-19) than adults; however, younger children (<4 years of age)¹ may develop more severe disease than older children. To date, the immune correlates of severe COVID-19 in young children have been poorly characterized. We report the kinetics of immune responses in relation to clinical and virological features in an infant with acute severe COVID-19. Systemic cellular and cytokine profiling showed initial increase in neutrophils and monocytes with depletion of lymphoid cell populations (particularly CD8+ T and NK cells) and elevated inflammatory cytokines. Expansion of memory CD4+T (but not CD8+T) cells occurred over time, with predominant Th2 bias. Marked activation of T cell populations observed during the acute infection gradually resolved as the child recovered. Significant in vitro activation of T-cell populations and robust cytokine production, in response to inactivated SARS-CoV-2 stimulation, was observed 3 months after infection indicating durable, long-lived cellular immune memory.

Main Text

A 4-month old male infant was transferred to The Royal Children's Hospital (RCH, Melbourne, Australia) with an acute respiratory illness early in the COVID-19 pandemic. He had cyanotic congenital heart disease with single ventricle physiology for which he had undergone partial correction with a systemic-to-pulmonary shunt inserted on day 8 of life. A day prior to presentation he developed low-grade fevers, cough and increased work of breathing. At his local hospital, he was hypoxic (initial oxygen saturation was 70%) and was commenced on low-flow nasal prong oxygen. His echo showed good ventricular function. Reverse-transcriptase-polymerase-chain-reaction (RT-PCR) for SARS-CoV-2 from a nasopharyngeal/oropharyngeal swab was positive. Both parents and a sibling had been diagnosed with COVID-19 in the preceding week.

The following day his respiratory status worsened and he developed severe respiratory and metabolic acidosis with pH 6.99, PCO₂ 55 mmHg and lactate 13 mmol/L. He was intubated and ventilated and transferred to the intensive care unit for further management (Figure 1A). He required mechanical ventilation with pressure support of 17cmH₂O and positive end-expiratory pressure of 8cmH₂O, respiratory rate of 25 breaths per minute and fraction inspired oxygen of 40%. There was evidence of haemodynamic compromise with relative bradycardia (heart rate 100 beats per minute), hypothermia (33 degrees Celsius) and hypotension (mean arterial blood pressure 35mmHg). He was commenced on an infusion of adrenaline 0.05 mcg/kg/min. A plain chest film showed peri-hilar interstitial and ground-glass opacities with left lower lobe collapse and small bilateral pleural effusions (Figure 1B). Notable initial laboratory investigations included elevated ferritin (9487 µg/L, normal range [NR 11-87) and d-dimers (5.86 µg/mL, NR <0.5) with reduced lymphocytes (0.43x10⁹/L, NR 4.0-10.0) (Supplementary Table 1).

He was treated with broad spectrum anti-microbials, intravenous immunoglobulin (1g/kg) and remdesivir (loading dose 5mg/kg then 2.5mg/kg then ceased as lyophilised solution was unavailable). Based on his cardiorespiratory deterioration and elevated inflammatory markers, therapies targeting the COVID-19

inflammatory response were administered, including tocilizumab 8mg/kg and dexamethasone 0.15mg/kg (twice daily for 5 days, Figure 1A). Anti-coagulation with low-molecular weight heparin was commenced to mitigate occlusion of his cardiac shunt.

Cycle threshold (Ct) values for SARS-CoV-2 in upper airway swabs were initially low (indicative of high viral load) with detectable viral RNA present until day 25. SARS-CoV-2 RT-PCR was positive in urine at day 3 of admission (Figure 1C); stool was negative at all time-points (Supplementary Table 2). Serology for SARS-CoV-2 S1 IgG, IgM and IgA was initially negative (day 3) with seroconversion occurring by day 5 and IgG and IgA remaining positive until day 84 (Figure 1D) indicating durable humoral immunity. Neutralising antibodies showed an early rise (days 3-5) with persistently high titres from day 10 through 28 (Figure 1D). A rapid decline in inflammatory markers (e.g. ferritin and IL-6, Figure 1E-F) was observed in association with clinical improvement and extubation occurred on day 5. Lymphocyte counts remained below normal reference ranges throughout admission and follow-up (Figure 1F).

Flow cytometry was performed on whole blood collected 3, 5, 10, 28 and 84 days following admission (Figure 2). Neutrophil and eosinophil proportions remained stable over the first 10 days. A substantial increase in both cell types was observed at day 28, with a 3.5-fold increase in neutrophils and a 12.8-fold increase in eosinophils (Figure 2A). Cells of lymphoid origin, including CD4⁺ T cells, CD8⁺ T cells, B cells and natural killer (NK) cells were markedly reduced at day 10, subsequently increasing (Figure 2A). Classical (CD14⁺CD16⁻) monocytes changed substantially over time, with marked increases observed at days 5, 10, 28, and 84 days after admission. Intermediate (CD14⁺CD16⁺) monocytes were virtually absent at day 3, increasing at days 5 and 10, with a decline observed by day 28 and returning by day 84. Non-classical (CD14^{low}CD16⁺) monocytes were essentially absent at the first three time points, returning to the circulation by day 84 (Figure 2A).

Unsupervised clustering analysis on whole blood flow cytometry data using FlowSOM² and UMAP³ was also performed. The frequency of clusters at each time point revealed identical sequential changes to that observed by manual gating and identified the presence of a CD16^{low} immature granulocyte cluster at day 3 and day 5 (Figure 2B). PBMCs were collected at each timepoint and used for high-dimensional flow cytometric analysis of T cell subsets as well as PBMCs from an age/sex matched infant who had undergone correction for a tetralogy of Fallot as a comparator (Figure 2B and Figure S1). $\gamma\delta$ TCR+V δ 2⁺ T-cells, which were much lower at day 3 compared to the control, increased more than ten-fold (0.22% at day 3 to 2.83% at day 84) (Figure 2C). Similarly, mucosal associated invariant T-cell (MAIT) frequencies had increased (0.2% to 0.35% from day 3 to day 84 respectively, Figure 2C). The proportion of Th2 cells, which were very low in the control child (2.36%), increased in the COVID-patient from 9.32% at day 3 to 28.2% at day 84, while the proportion of Th1, Th17 or Treg populations varied little over time (Figure 2D). Effector and central memory CD4⁺ T-cell subsets expanded from day 3 onwards, however this was not seen for CD8⁺ T-cells (Figure 2D). CD69, a marker used to define activated T cells, was minimally expressed on the control PBMC sample (Figure 2E). In contrast, high CD69 expression was observed on CD4⁺T cells, CD8⁺T cells, $\gamma\delta$ TCR+V δ 2⁺ T-cells and MAIT cells at day 3 (Figure 2E). CD69 expression on

these T-cell subsets gradually declined after day 3 to levels akin to the control, although CD69+ expression on MAIT cells increased again by day 84 (Figure 2E).

Multiplex analysis of serum samples revealed a broad array of cytokines produced throughout the course of infection (Figure 2F). The acute phase was dominated by inflammatory cytokines such as IL-6, IL-8 and TNF α and the chemokine IP-10 (CXCL10) at day 3 (Figure 2F), consistent with previous data from severe COVID-19 disease in adults.⁴⁻⁷ In addition, IFN γ , G-CSF, Eotaxin, MIP-1 α and MCP-1 were also highly elevated at this time-point compared to later time-points (Figure 2F), indicative of a potent pro-inflammatory immune response and enhanced cell migration. The level of IL-6 was markedly reduced by day 5 after tocilizumab (anti-IL-6) therapy and remained low at subsequent time-points (Figure 2F). Furthermore, early treatment with remdesivir, tocilizumab and dexamethasone (and/or natural history of COVID-19 infection) correlated with a shift towards Th2-type anti-inflammatory cytokines (e.g IL-4, IL-5, IL-10, IL-13) by day 10. However, high levels of PPGF-BB, IL-1b, IL-2, IL-7, IL-15 and IL-17 were also observed at this time coinciding with disease resolution (Figure 2F). This cytokine profile correlated with the early activation of immune cells observed at day 3 (Figure 2F). By day 28, high levels of IL-1b and IL-15 were observed, while day 84 was characterised by increased IL-9, MIP-1 β and RANTES (Regulated on Activation, Normal T cell expressed and Secreted, Figure 2F).

Interestingly, we also found IL-18 was highest on day 3 (Figure 2F) which correlated with greatest CD69 activation on both Vd2+ gd T cells and MAIT cells (Figure 2E). Moreover, whilst IL-12 was predominantly detected at day 10, both IL-18 and IL-12 were detected at day 84 (Figure 1F) correlating with high CD69 expression on MAIT cells at this time-point. Innate-like T-cells, such as Vd2+ gd T cells and MAIT cells have been implicated in anti-viral immunity.⁸⁻¹⁰ Activation of these cells by viruses is thought to occur via T-cell receptor (TCR) independent mechanisms, through IL-12 and IL-18 stimulation.⁸⁻¹⁰

To examine the memory T cell response, PBMCs from the control infant and COVID-infected infant (day 84) were stimulated with inactivated SARS-CoV-2 (Figure 3). A substantial increase in CD69 expression was observed in CD4+ (27.2%) and CD8+ (20.2%) T-cells compared to the age/sex-matched control (<5%) (Figure 3A). This was accompanied by robust production of both pro- and anti-inflammatory cytokines and chemokines (IL-2, IL-4, IL-5, IL-6, IL-9, IL-10, IL-13, IL-15, IL-17, IFN γ , IP-10, TNF α) in PBMC supernatants, which was not observed in our control patient (Figure 3B and Supplementary Figure 4). These data reveal a strong memory T cell response to SARS-CoV-2, suggestive of long-lasting protective T cell-mediated immunity.

We have provided comprehensive longitudinal analyses of the clinical, immunological and virological findings in an infant with severe COVID-19. Overall, our cellular and cytokine findings support previous studies demonstrating depletion of lymphoid and innate cell populations in the early phase of severe COVID-19.¹¹⁻¹³ We report several novel findings in this infant with severe COVID-19. First, the immune response was characterised by early and marked alterations in neutrophil and monocyte populations, expansion of CD4+ (but not CD8+) T cell populations coinciding with robust antibody responses, activation of innate-like immune cells (e.g. CD69+ MAIT cells) and Th2 and IL17 cytokine skewing.

Second, robust and enduring memory T cell responses were maintained for at least 84 days, suggesting functional immune memory. Third, activation of innate-like T cells was observed. This is consistent with studies in adults showing MAIT cell activation in severe COVID-19,¹⁴ suggesting it may also represent a biomarker for severe COVID-19 infection in children. Overall, the findings support long-lived cellular immunity to SARS-CoV-2 infection and may inform future research into preventative interventions and therapeutic targets for severe COVID-19 in children.

Declarations

Acknowledgements

We acknowledge this child's family for their contribution to this research. We also acknowledge the Clinical Laboratory team at The Royal Children's Hospital, Melbourne for their support.

Author contributions

These authors contributed equally: Danielle Wurzel, Melanie Neeland, Jeremy Anderson.

These authors jointly supervised this work: Nigel Crawford, Paul Licciardi, Trevor Duke, Daniel Pellicci.

DFW co-conceptualised the study, contributed to analyses and co-wrote the manuscript with MN and JA. MN, JA, ZT, RH, LD, CD, LAHD planned, performed and analysed the experiments with the assistance of PVL, DGP, JB, SJ; TD, TC, DB, AD, JB, SM, GH, AS, KS, VC, AD, LL, PB, LYL, YNA and ST provided clinical expertise and contributed to data interpretation. AA, AM, KD, IO and IK collected and/or processed patient samples and assisted with manuscript preparation. NC conceptualized the study and drafted the manuscript.

Competing interests

The authors declare no competing interests.

Ethics statement:

Ethics approval for this study was granted by the Royal Children's Hospital Human Research Ethics Committee (HREC approval #63103). Written informed consent was obtained electronically from the child's parents/guardians.

Funding:

This study was funded by Murdoch Children's Research Institute COVID-19 research program; Centers of Excellence in Influenza Research and Surveillance - Cross-Center Southern Hemisphere Project, National Institute of Health (NIH); The Influenza Complications Alert Network Surveillance System (FluCAN); Paediatric Active Enhanced Disease Surveillance (PAEDS) and Sentinel Travelers and Research Preparedness Platform for Emerging Infectious Disease (SETREP-ID) - Australian Partnership for

Preparedness Research on Infectious Disease Emergencies. Funding was also provided through the Victoria Government's Operational Infrastructure Support Program. PVL is supported by Australian National Health and Medical Research Council (NHMRC) Career Development Fellowship. DGP is supported by a CSL Centenary Fellowship.

References

1. Leidman, E., *et al.* COVID-19 Trends Among Persons Aged 0–24 Years – United States, March 1–December 12, 2020. *MMWR Morb Mortal Wkly Rep*, 88-94 (2021).
2. Van Gassen, S., *et al.* FlowSOM: Using self-organizing maps for visualization and interpretation of cytometry data. *Cytometry A***87**, 636-645 (2015).
3. McInnes, L., Healy, J. & Melville, J. UMAP: Uniform Manifold Approximation and Projection for Dimension Reduction. *arXiv e-prints arXiv:1802.03426* (2018).
4. Del Valle, D.M., *et al.* An inflammatory cytokine signature predicts COVID-19 severity and survival. *Nature Medicine***26**, 1636-1643 (2020).
5. Laing, A.G., *et al.* A dynamic COVID-19 immune signature includes associations with poor prognosis. *Nature Medicine***26**, 1623-1635 (2020).
6. Lucas, C., *et al.* Longitudinal analyses reveal immunological misfiring in severe COVID-19. *Nature***584**, 463-469 (2020).
7. Rydyznski Moderbacher, C., *et al.* Antigen-Specific Adaptive Immunity to SARS-CoV-2 in Acute COVID-19 and Associations with Age and Disease Severity. *Cell***183**, 996-1012.e1019 (2020).
8. Ussher, J.E., *et al.* CD161⁺⁺ CD8⁺ T cells, including the MAIT cell subset, are specifically activated by IL-12+IL-18 in a TCR-independent manner. *Eur J Immunol***44**, 195-203 (2014).
9. Ussher, J.E., Willberg, C.B. & Klenerman, P. MAIT cells and viruses. *Immunol Cell Bio***96**, 630-641 (2018).
10. van Wilgenburg, B., *et al.* MAIT cells are activated during human viral infections. *Nature Communications***7**, 11653 (2016).
11. Chen, G., *et al.* Clinical and immunological features of severe and moderate coronavirus disease 2019. *J Clin Invest***130**, 2620-2629 (2020).
12. Sun, H.B., *et al.* The changes of the peripheral CD4⁺ lymphocytes and inflammatory cytokines in Patients with COVID-19. *PLoS One***15**, e0239532 (2020).
13. Zhang, X., *et al.* Viral and host factors related to the clinical outcome of COVID-19. *Nature***583**, 437-440 (2020).
14. Parrot, T., *et al.* MAIT cell activation and dynamics associated with COVID-19 disease severity. *Sci Immunol***5**(2020).
15. Cowley, D., Donato, C.M., Roczo-Farkas, S. & Kirkwood, C.D. Novel G10P[14] rotavirus strain, northern territory, Australia. *Emerg Infect Dis***19**, 1324-1327 (2013).

16. Chan, J.F., *et al.* Improved Molecular Diagnosis of COVID-19 by the Novel, Highly Sensitive and Specific COVID-19-RdRp/HeI Real-Time Reverse Transcription-PCR Assay Validated In Vitro and with Clinical Specimens. *J Clin Microbiol* **58**(2020).
17. Corman, V.M., *et al.* Detection of 2019 novel coronavirus (2019-nCoV) by real-time RT-PCR. *Euro Surveill* **25**(2020).

Figures

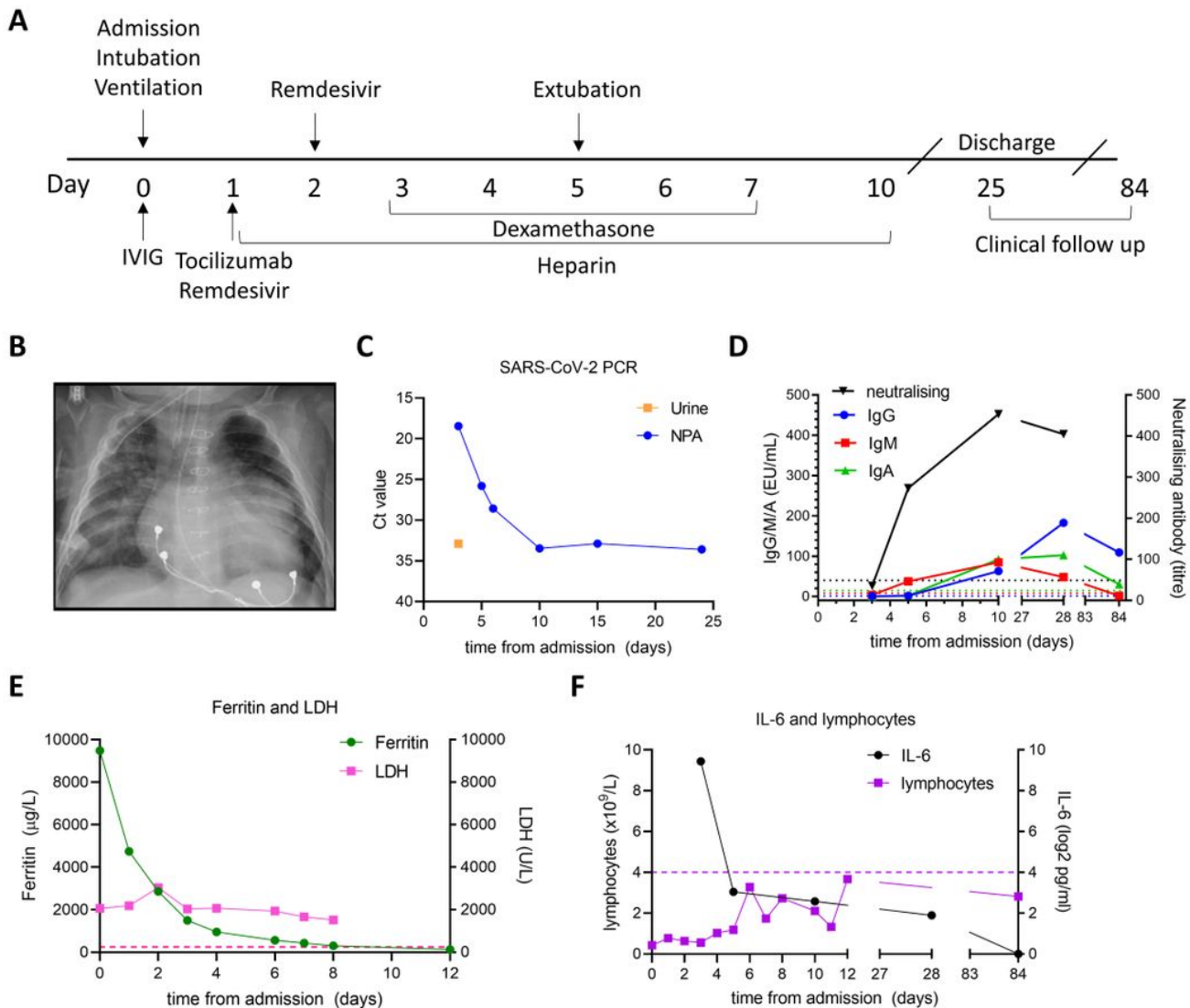


Figure 1

Clinical and laboratory characteristics of an infant with severe COVID-19 (A) Clinical timeline showing immuno-modulatory therapies in relation to clinical course. (B) Plain chest film performed on admission illustrating bilateral interstitial infiltrates with left lower lobe collapse and consolidation. (C) Virologic findings illustrating SARS-CoV-2 Cycle threshold Ct values in naso-/oropharyngeal, stool and urine specimens which reduce in association with clinical improvement (D) Serum IgG, IgM and IgA to S1 using

in-house ELISA modified from Mount Sinai Laboratories, USA; and microneutralisation assay demonstrating rapid rise in neutralising antibody titres (E) Elevated ferritin and LDH with initial hyper-inflammatory picture and rapid reduction in ferritin coinciding with clinical improvement (F) Persistent lymphopaenia; initial high IL-6 with reduction after administration of tocilizumab. IVIG = intravenous immunoglobulin.

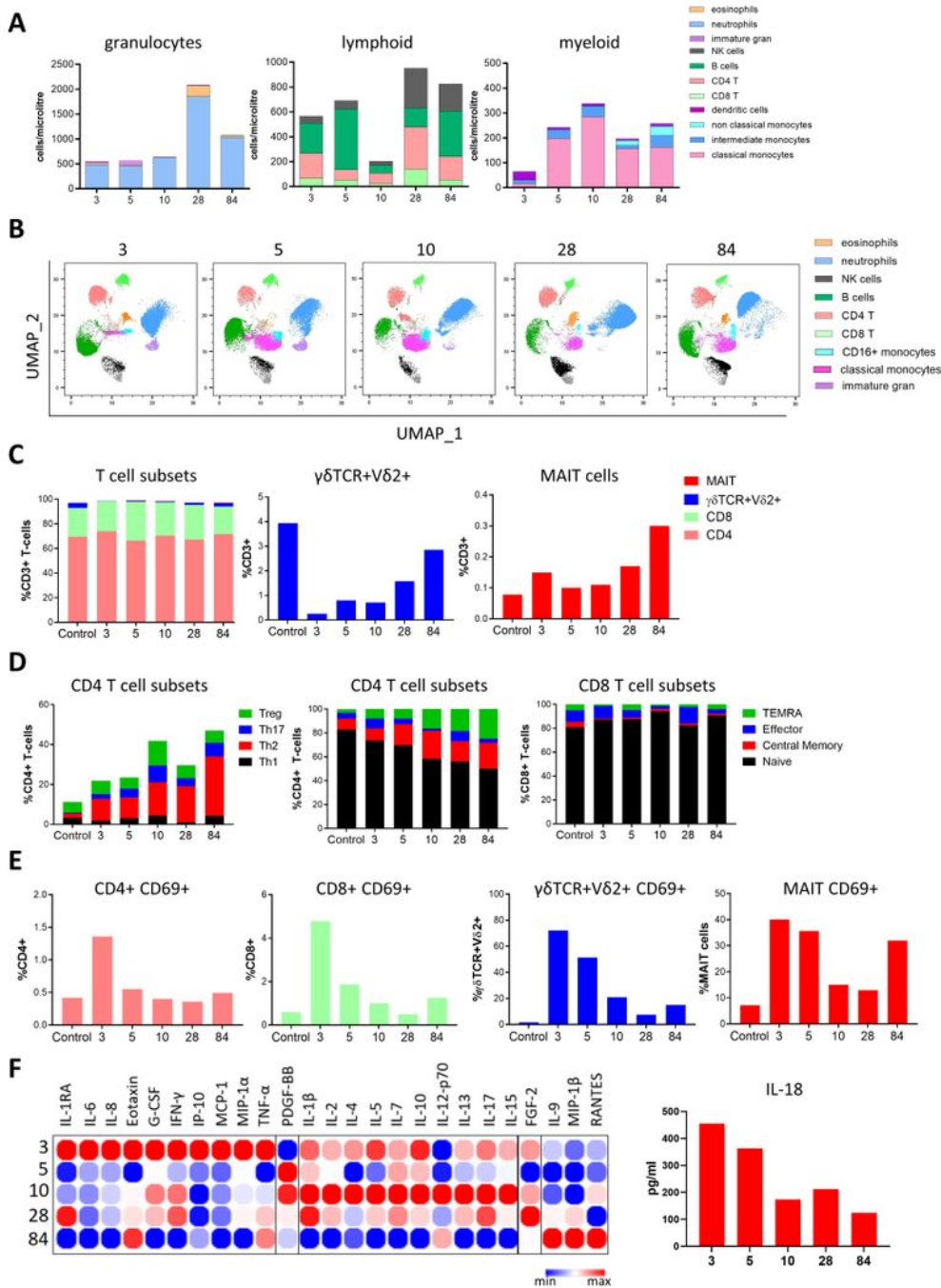


Figure 2

Immune cell profiling in whole blood and PBMCs (A) Flow cytometry was performed on whole blood samples collected at 3, 5, 10, 28, and 84 days following admission. Neutrophils, eosinophils, CD4 T cells, CD8 T cells, B cells, Natural Killer (NK) cells, monocytes (classical, intermediate and non-classical) and dendritic cells were classified by manual gating and expressed as cells/ μ L using counting beads. (B) Unsupervised clustering and dimensionality reduction were performed using FlowSOM and UMAP on a concatenated file containing 150,000 live single cells (30,000 randomly selected cells from each time point). The UMAP plots at each time point are coloured according to the generated FlowSOM clusters. (C) Flow cytometry was performed on peripheral blood mononuclear cells collected on days 3, 5, 10, 28 and 84 following admission. CD4, CD8, $\gamma\delta$ V δ 2+ T-cells and MAIT cells were classified by manual gating and expressed as frequency of CD3+ T-cells. These results were compared to an age/sex matched control (D) Subsets of CD4+ and CD8+ T-cells were further categorised by flow cytometry to determine frequency of Th1, Th2, Th17, Treg and memory subsets. These were expressed as the frequency of CD4+ or CD8+ T-cells. (E) Flow cytometry was performed to assess activation status of T-cells. CD69+ was expressed as a proportion of total CD4+, CD8+, $\gamma\delta$ V δ 2+ T-cells and MAIT cells. (F) Cytokines were quantified in the serum using a multiplex cytokine assay and visualised in a heatmap containing log2 transformed values and clustered according to peak expression at day 3 (cluster 1), day 5 (cluster 2), day 10 (cluster 3) and day 28 (cluster 4). IL-18 levels at days 3, 5, 10, 28 and 84 were quantified by ELISA and expressed as pg/ml.

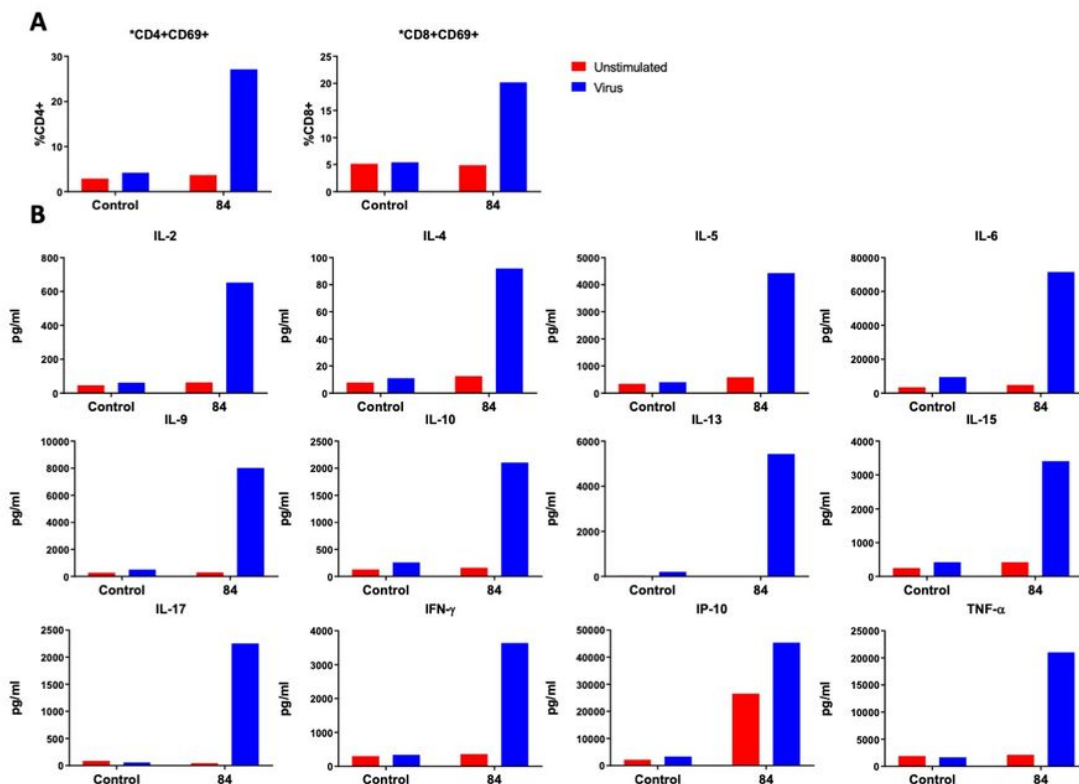


Figure 3

Immune response to inactivated SARS-CoV-2 (A) Flow cytometry was performed on PBMCs following 4-day stimulation with inactivated SARS-CoV-2 to observe T-cell activation status. CD69+ was expressed as a proportion of total CD4+ or CD8+ T-cells. (B) Cytokines were quantified in PBMC supernatants following

4-day stimulation with inactivated SARS-CoV-2 by multiplex cytokine assay to assess memory T-cell responses.

Supplementary Files

This is a list of supplementary files associated with this preprint. Click to download.

- [WURZELetalsupplementNatureMedComm.docx](#)